Deep-Sea Research Part II 165 (2019) 192–202

Contents lists available at ScienceDirect

Deep-Sea Research Part II

journal homepage: www.elsevier.com/locate/dsr2

Microzooplankton in the coastal Gulf of Alaska: Regional, seasonal and interannual variations

Suzanne L. Strom*, Kerri A. Fredrickson, Kelley J. Bright

Shannon Point Marine Center, Western Washington University, 1900 Shannon Point Rd., Anacortes, WA 98221, United States

ARTICLE INFO

Keywords:
Ciliates
Dinoflagellates
Microzooplankton
Coastal Gulf of Alaska
Planktonic food web

ABSTRACT

Microzooplankton communities in the coastal Gulf of Alaska (CGOA) were studied during two contrasting years: 2011, with a greatly reduced spring phytoplankton bloom, and 2013, with a robust spring bloom. Other sampling contrasts were season (spring, summer, fall) and region (eastern versus western shelf waters). Ciliates and dinoflagellates comprised nearly all microzooplankton in the ≥ 15 µm size class. Many of the strongest contrasts in the biomass and taxonomic composition of the microzooplankton community were regional. The east had generally lower microzooplankton biomass levels and a greater proportion of ciliates than the west, even in the face of basin-wide seasonal and interannual contrasts. This difference is likely a consequence of the narrower shelf in the east, which leads to a lower productivity environment. Interannual differences in spring bloom intensity were reflected in microzooplankton biomass (higher in spring 2013, especially in the east), while interannual differences in taxonomic composition persisted throughout the year, with a greater representation of ciliates in 2011. Ciliate dominance could reflect adaptations to lower productivity conditions, with many of the largest taxa likely retaining chloroplasts as a strategy (mixotrophy) for survival during times of prey scarcity. Microzooplankton: phytoplankton biomass ratios varied widely over time and space. These ratios indicate that lower productivity regions (east) and seasons (summer) also tend to be locations and times of reduced trophic transfer efficiency from phytoplankton to ciliates and dinoflagellates. Ciliates and dinoflagellates can be preferred prey of mesozooplankton, including dominant CGOA copepod species. Thus multiple mechanisms conspire to reduce the flow of matter and energy to higher trophic levels in low productivity locations and time periods in the CGOA.

1. Introduction

The activities of microzooplankton are integral to marine planktonic ecosystems. As the main consumers of phytoplankton in both coastal and oceanic waters (Calbet and Landry, 2004; Schmoker et al., 2013), microzooplankton are significant regenerators of the nutrients that fuel primary production, and form a key trophic link between phytoplankton and metazoans including copepods and larval fish. Here we focus primarily on ≥ 15 µm phagotrophic protists (mainly dinoflagellates and ciliates); this is the size class most efficiently consumed by the crustacean zooplankton that are important trophic intermediaries in the productive CGOA ecosystem (e.g. Liu et al., 2005; Pinchuk and Hopcroft, 2006).

Despite their ecological importance, microzooplankton communities remain substantially understudied relative to most other functional groups in the plankton. In the coastal Gulf of Alaska (CGOA), previous investigations have reported a wide range of biomass, with some of the highest occurring during spring phytoplankton blooms. On the Seward Line in the northern CGOA (Fig. 1), experimental work in spring and summer showed that microzooplankton grazers consumed nearly all production by small phytoplankton, and an average of half the production in the larger (diatom) size fraction (Strom et al., 2007). Trophic linkages to mesozooplankton are also significant in this region. *Neocalanus* spp., which dominate the CGOA copepod biomass in spring, exhibited high clearance rates on microzooplankton, especially the largest ciliates and dinoflagellates (Dagg et al., 2009). Microzooplankton can also contribute substantially to the diet of summer-dominant CGOA copepods such as *Pseudocalanus* spp., (J. Napp, personal communication). Although data for CGOA species are lacking, in general microzooplankton are also fed upon by some larval fish species, and could be especially important during nutritionally critical first-feeding stages (reviewed by Montagnes et al., 2010).

Planktonic food webs in the CGOA are profoundly influenced by the physical and meteorological setting. The moderately productive

* Corresponding author.
E-mail address: Suzanne.Strom@wwu.edu (S.L. Strom).

https://doi.org/10.1016/j.dsr2.2018.07.012

Available online 27 July 2018
0967-0645/ © 2018 Elsevier Ltd. All rights reserved.

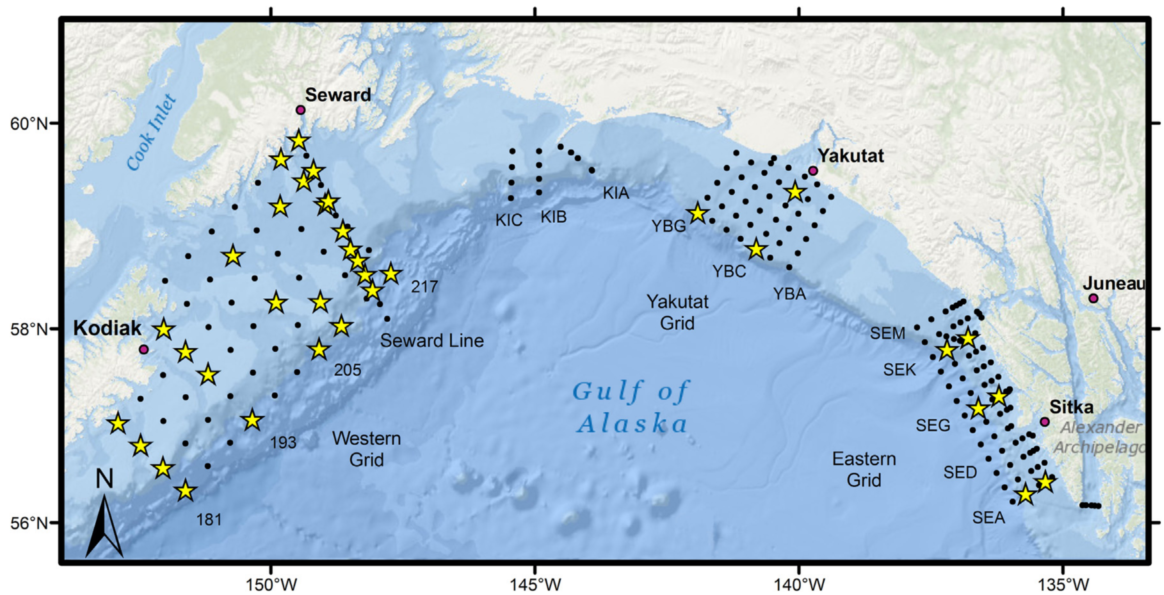

Fig. 1. Map of coastal Gulf of Alaska study region, showing GOA-IERP sampling grids (black dots) and stations where microzooplankton data for this publication were collected (stars). Seward Line and Western Grid comprise 'west' region, while Yakutat and Eastern Grid comprise 'east' region.

continental shelf adjoins open seas in which phytoplankton production is chronically iron-limited (Boyd et al., 2004), giving rise to strong cross-shelf gradients in planktonic community structure (Coyle and Pinchuk, 2005; Strom et al., 2006, 2007). The shelf is cross-cut by canyons carved during the last glacial maximum, and the mountainous coastline is intersected by numerous bays, sounds, and entrances. Coupled with episodically strong winds and extremely high freshwater inputs, these features lead to a vigorous coastal circulation regime that includes a coastally trapped alongshore current (the Alaska Coastal Current, or ACC), seasonally alternating strong downwelling and weak upwelling, and episodic formation of mesoscale eddies, particularly in the east (Stabeno et al., 2004; Weingartner, 2005). This constellation of features, along with highly variable weather patterns, gives rise to a coastal ecosystem in which bottom-up regulation of primary production is mediated by a mosaic of potential limiting factors including light, macronutrients, and iron (Fiechter et al., 2009; Strom et al., 2016, 2010, 2006; Wu et al., 2009).

Numerous modeling approaches have been applied to better understand the CGOA ecosystem, including plankton dynamics models coupled to representations of the 3-D circulation (Coyle et al., 2012, 2013; Fiechter and Moore, 2009; Fiechter et al., 2009; Hinckley et al., 2009), and a variety of static food web models focused on different trophic levels or functional groups (Aydin et al., 2005; Gaichas et al., 2010; Ruzicka et al., 2013). Owing to the magnitude of material and energy flows through the lowest trophic levels, predictions of higher trophic level production are highly sensitive to inclusion and parameterization of the microzooplankton trophic link (e.g. Aydin et al., 2005). Data on biomass and community composition are likewise required for ground-truthing of these predictive tools (e.g. Fiechter and Moore, 2009). However, data on microzooplankton are scarce for the CGOA.

As part of the larger Gulf of Alaska – Integrated Ecosystem Research Program (GOA-IERP), our goals were to measure abundance and biomass, and to evaluate the taxonomic and size composition of the CGOA microzooplankton community. GOA-IERP overall was designed to assess planktonic ecosystem structure across three potential gradients: regional (east versus west coastal waters); seasonal (spring, summer, fall); and interannual (2011 versus 2013). A better understanding of lower trophic level food web structure will inform conceptual and numerical models of this dynamic ecosystem, including those that address the intense variability in recruitment of commercially valuable GOA groundfish species.

2. Materials and methods

2.1. Field sampling

Microzooplankton samples, along with accompanying environmental data, were collected on 14 oceanographic cruises to the coastal Gulf of Alaska as part of the GOA-IERP 2011 and 2013 field seasons (Table 1). Stations selected for microzooplankton sampling and analysis comprised a subset of the overall program station grid (Fig. 1). Water samples for chlorophyll and microzooplankton determination were collected with Niskin bottles as part of the CTD package on each vessel. Chlorophyll sampling and analysis methods are described in Strom et al. (2016). Microzooplankton samples were collected from 10, 20, 30 and 50 m (and occasionally from the surface); seawater was gently drained through silicone tubing into amber glass bottles pre-loaded

Table 1
Cruises and time periods from which microzooplankton samples were obtained during the GOA-IERP project. n = number of microzooplankton samples analyzed for this publication from 10 m depth, and in total (in parentheses, if different from 10 m total). Analyses presented here are based primarily on 10 m samples.

Year/Season	Vessel	Cruise Dates	Region	n
2011				
Spring	*Thomas G. Thompson*	4/30 – 5/21	east	10 (34)
	Tiglax	4/26 – 5/11	west	16 (22)
Summer	*Northwest Explorer*	6/30 – 7/24	east	6 (12)
	Northwest Explorer	7/30 – 8/22	west	11 (14)
Fall	*Northwest Explorer*	9/3 – 9/25	east	6 (9)
	Tiglax	9/14 – 9/20	west[a]	5
	Northwest Explorer	9/25 – 10/9	west	6
2013				
Spring	*Oscar Dyson*	4/4 – 4/24	east	8
	Tiglax	4/25 – 5/9	west	11
Summer	*Northwest Explorer*	7/3 – 7/21	east	6
	Northwest Explorer	8/3 – 8/22	west	8
Fall	*Tiglax*	9/13 – 9/18	east	6
	Tiglax	9/23 – 9/26	west[a]	6
	Oscar Dyson	9/24 – 9/30	west	5

[a] Seward Line only (see Fig. 1).

with acid Lugol's solution, taking care to submerge the drain tube in the fixative and to avoid bubbling. Final acid Lugol's concentration was 5%.

2.2. Microzooplankton and nanoflagellate sample analysis

For microzooplankton, sample volumes ranging from 10 to 100 ml were settled (larger volumes using a two-stage settling process) and cells enumerated using inverted microscopy at 250 x. In all but a few samples, > 150 cells were counted, identified and measured; in most cases the total was > 200. All ciliates regardless of size, and all dinoflagellates ≥ 20 µm, were assigned to a general taxonomic and shape category, then measured using a computer-linked digitizing pad and Microbiota software (Roff and Hopcroft, 1986). Broad taxonomic categories for ciliates included tintinnids, the chloroplast-retaining species *Laboea strobila*, and all other oligotrichs (= aloricate choreotrichs). For dinoflagellates, we distinguished athecate forms in the *Gymnodinium/Gyrodinium* complex, thecate forms including *Protoperidinium* and related genera, and other (generally thecate) species. Copepod nauplii and other invertebrate larvae were occasionally noted, but could not be reliably quantified from these sample volumes. Microzooplankton cell volumes were computed from measured dimensions and assigned shapes. Carbon biomass was estimated from cell volume based on published conversion factors obtained for acid Lugol's-fixed cells. For ciliates, we assumed a constant 0.19 pg C μm^{-3} (Putt and Stoecker, 1989); for dinoflagellates, C content scaled with cell volume according to log pg C $cell^{-1}$ = -0.119 + 0.819(logV) where V = cell volume in μm^3 (Menden-Deuer and Lessard, 2000).

Dinoflagellates < 20 µm and heterotrophic nanoflagellates were enumerated at a subset of microzooplankton stations. Water samples from CTD casts were prescreened (100 µm) into bottles preloaded with glutaraldehyde (final concentration 0.5%) and DAPI stain, refrigerated approximately 24 h, then filtered (0.8 µm pore size polycarbonate with 1.2 µm backing filter), slide-mounted using low fluorescence immersion oil, and stored at −80 °C. Slides were returned to the shore laboratory on dry ice and examined within 6 months of collection using epifluorescence microscopy with UV and blue excitation to distinguish nuclear morphology and chlorophyll autofluorescence, respectively. Flagellates were placed into shape and size classes and C biomass (pg $cell^{-1}$) estimated from calculated biovolume (BV) using the relationship of Verity et al. (1992): logC = -0.363 + 0.863(logBV).

2.3. Phytoplankton biomass estimation

Chlorophyll *a* concentrations (Chl) were converted to carbon using C:Chl measured during spring of both years in the eastern grid during this program (Strom et al., 2016), or measured along the Seward Line during monthly sampling by the U.S. GLOBEC program during 2001 and 2003 (Coyle et al., 2012; their Fig. 7). For the latter, samples collected at station GAK-12 were excluded as likely representative of oceanic (rather than shelf) plankton communities. During spring, we measured the C:Chl of the < 20 µm size fraction only (Table 2); median ratios were 76 (in 2011) and 41 (in 2013). For the > 20 µm size fraction in spring of both years, we used the spring mean from Coyle et al. (2012) of 36. For summer and fall, no distinction was made between Chl size fractions due to lack of data and again, mean seasonal values were used (Table 2). Ultimately, phytoplankton C estimates were used with microzooplankton biomass estimates from the same water samples to calculate C-based microzooplankton: phytoplankton biomass ratios (MZ:P).

2.4. Statistical analysis

Principal components analysis (PCA) was conducted on the pooled (both years, all regions and seasons) data set consisting of 11 distinct size/taxonomic categories of microzooplankton from 10 m samples. PCA was done in PRIMER v.6 on log-transformed C biomass data. We used the broken-stick model (Jackson, 1993) to assess the significance of each principal component. We also investigated relationships between environmental variables (temperature, salinity, macronutrient concentrations, Chl) and microzooplankton community patterns using the BIO-ENV package in PRIMER. Environmental data were normalized (to a mean of 0 and a standard deviation of 1) to afford them equal weight in the analysis. Correlation analysis was conducted in SPSS v.20.

Table 2
Summary of phytoplankton community characteristics, by region (east versus west) and chlorophyll size fraction (SF, total, < 20 or > 20 µm) during GOA-IERP cruises to the coastal Gulf of Alaska. Shown are depth-integrated chlorophyll concentration (Chl(int), mg m^{-2}, 0–50 m), the fraction of total integrated chlorophyll found in the > 20 µm size fraction (SF > 20), and the phytoplankton carbon:chlorophyll ratio (C:Chl, wt:wt). Median values are shown; n = 23 – 70 for Chl(int) and SF > 20; n = 13 – 17 for GOA-IERP C:Chl estimates. Unless otherwise indicated, C:Chl ratios (wt:wt) were taken from Coyle et al. (2012). nd = not determined.

	Region	SF	2011			2013		
			spring	summer	fall	spring	summer	fall
Chl(int)	E	total	29.4	25.2	33.1	61.7	29.6	29.0
	W	total	38.4	34.5	33.0	217.0	34.7	32.2
SF > 20	E		0.09	nd	nd	0.73	nd	0.06
	W		0.43	nd	nd	0.88	nd	0.17
C: Chl	all	< 20	76[a]	53	33	41[a]	53	33
	all	> 20	36	53	33	36	53	33

[a] C:Chl ratios measured on GOA-IERP cruises (see Strom et al. 2016 for methods).

3. Results

3.1. Microzooplankton abundance and biomass

Microzooplankton abundance across all samples ranged from 0.9 to 57.2 × 10^3 cells $liter^{-1}$ (median = 12.9 × 10^3; mean = 14.8 × 10^3; Table S1). The overall range of 10-m microzooplankton biomass across all seasons and regions was 1.3 – 92.7 µg C $liter^{-1}$. With the exception of the eastern region in 2011, a seasonal cycle was apparent for each region and year, with highest median biomasses in spring followed by ~ 2-fold declines to approximately equivalent values for summer and fall (Fig. 2a,b). In general the highest microzooplankton biomass was encountered near shore with declining stocks over the outer shelf and slope (Fig. 3), although exceptions were sometimes observed.

The western region always had a higher median and maximum 10-m biomass than the east (Fig. 2a,b). With the exception of spring 2011, when differences were even more pronounced, medians in the west were 2–3x higher than those in the east for any given season and year. An interannual difference in biomass was apparent only in spring, and was particularly pronounced in the east. Median biomass in spring 2011 was only 5.3 µg C $liter^{-1}$ in the east, in comparison with the spring 2013 median of 18.0 µg C $liter^{-1}$. These low spring values obviated the seasonal biomass cycle in the eastern region during 2011.

Based on the subset of stations for which a full depth profile was analyzed, depth-integrated microzooplankton biomass was strongly predicted by the biomass at 10 m (Fig. 4). We used this relationship to estimate integrated biomass (mg C m^{-2}; 0–50 m) from 10-m data at all sampled stations (Fig. 1) during both years. Predicted integrated biomass ranged from 50 to 4290 mg C m^{-2} in 2011, with a median of 440 and a mean of 750 mg C m^{-2}. In 2013, predicted integrated biomass ranged from 3 to 3220 mg C m^{-2}. Measures of central tendency were higher in 2013, with a median of 600 and a mean of 820 mg C m^{-2}.

3.2. Microzooplankton community composition

Community composition (by biomass) ranged from almost complete

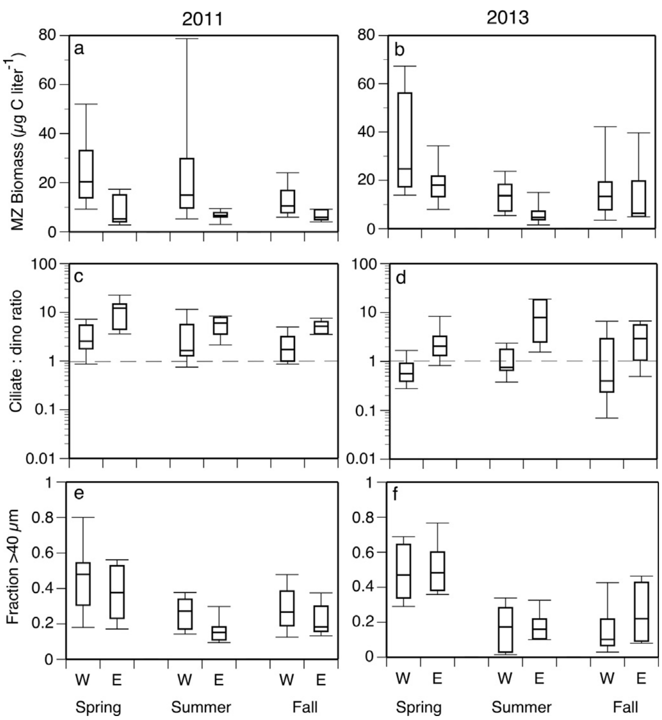

Fig. 2. Box plots of microzooplankton biomass (a, b), ciliate:dinoflagellate biomass ratio (c, d), and fraction of total microzooplankton biomass in cells > 40 µm (e, f) for western and eastern regions during 3 seasons in 2011 (left panels) and 2013 (right panels). All data from 10 m samples. Top, bottom and line through center of boxes denote 75th percentile, median (50th percentile) and 25th percentile of the data, respectively. Whiskers extend from the 10th percentile to the 90th. Dashed horizontal lines in c and d indicate 1:1 ratio.

dominance by ciliates (e.g. spring 2011; Fig. 3A) to a high proportion of dinoflagellates (e.g. spring 2013 in the west; Fig. 3B). Two major trends in community composition are apparent. First, the western region consistently had a lower proportion of ciliates than the east; that is, the west was always richer in dinoflagellate biomass regardless of season or year (Fig. 2c,d). Second, across the entire CGOA, 2011 was generally more ciliate-dominated than 2013, an interannual difference that was especially pronounced in the west (Fig. 3).

As for microzooplankton biomass, the size composition of the community showed strong seasonality. Median size was largest in spring, when the highest fraction of large (> 40 µm) cells was consistently observed (Fig. 2e,f; Fig. 3). During spring the peak ESD in both regions was between 14 and 18 µm except for 2011 in the east, when it was slightly smaller (Fig. 5a). (Note that, while ESD is a good representation of relative cell volumes, it understates the maximum dimension of most cells, which were typically not spherical.) During summer and fall, microzooplankton ESD shifted to smaller sizes (Fig. 5b,c). An unusual feature was the very high incidence of cells ~10 µm in ESD during summer 2013 in the west (Fig. 5b). However, consistent cell size differences between the regions were not apparent. The largest interannual differences in size composition were seen in the spring, when the size frequency distribution for both regions was shifted toward smaller cells in 2011 (Fig. 5a).

As a further indication of interannual differences in the microzooplankton community, we analyzed spring 10-m samples from the eastern region (stations on the Eastern and Yakutat grids) for the composition and biomass of the smallest heterotrophic protists, the < 20 µm flagellates. This community comprised both heterotrophic dinoflagellates (hdino) and a mix of other heterotrophic nanoflagellate taxa (hflag) that were not further differentiated in our study. Both the biomass and the composition of this community differed between the two years. In spring 2011, the median biomass for all < 20 µm heterotrophic protists was 9.7 µg C liter^{-1}, while the average was 12.5 µg C liter^{-1} (n = 28). In general, hdinos were the main constituent (median hflag/hdino biomass ratio = 0.4). Biomass of this flagellate community was much lower in spring 2013, with a median of 3.9 µg C liter^{-1} and an average of 4.6 µg C liter^{-1} (n = 23). Composition differed as well, with hflag rather than hdino the major constituent (median hflag/hdino biomass ratio = 3.9).

Comparing the < 20 µm flagellate biomass to that of the larger microzooplankton reveals further interannual contrasts. In spring 2011, the < 20 µm flagellates were always a substantial component of the total (microzooplankton + < 20 flagellate) biomass (Table 3). In contrast, the spring 2013 community comprised mainly the larger microzooplankton, with the < 20 µm flagellates amounting to < 20% of the total in all but one case. Thus for the eastern region, the general picture is one of a protist grazer community shifted to dominance by the smallest members (< 20 µm flagellates) in the low-chlorophyll spring of 2011, while during the high-chlorophyll spring of 2013, the protist grazer community was mainly composed of larger ciliates and dinoflagellates.

Note that the exclusion of flagellates < 20 µm from our routine microzooplankton biomass estimates, while standard practice in the field due to methodological limitations, has several implications for understanding lower trophic level ecology in the CGOA. Firstly, where samples for epifluorescence microscopy were not collected, we clearly missed a potentially sizeable component of the heterotrophic dinoflagellate community, especially during low production time periods (Table 2). These smaller dinoflagellates likely feed mainly on pico- and nanophytoplankton (e.g. Sherr et al., 1991; Strom, 1991); therefore, a portion of the phytoplankton grazer community is not included in our overall analysis of microzooplankton biomass patterns. Secondly, for the same reason (herbivory by < 20 µm dino- and nanoflagellates), the microzooplankton community described here is not strictly comparable to that responsible for community grazing rates as estimated by the seawater dilution technique in these waters (e.g. Strom et al., 2007). However, out analysis does capture the dynamics of the community most readily consumed by larger zooplankton, as well as that most likely to crop the spring bloom.

As we concurrently observed for phytoplankton (Strom et al., 2016), increases in total microzooplankton biomass were strongly driven by increases in the biomass of the larger size class of cells, especially during spring (Fig. 6). In 2011, these larger cells were mainly ciliates. For high biomass samples (total microzooplankton > 20 µg C liter^{-1}), the > 40 µm community in 2011 averaged 79% ciliates by biomass. In contrast, dinoflagellates played a greater role in 2013, averaging 53% of the > 40 µm community in high biomass samples. Thus composition of the large-celled component of the microzooplankton community changed substantially – from ciliate to dinoflagellate dominance - between 2011 and 2013.

3.3. Broad-scale patterns in phyto- and microzooplankton

Median MZ:P carbon biomass ratios for a given region, season and year ranged from 0.05 (east in summer 2013) to 0.36 (west in summer and fall 2011). Variability in MZ:P was high, as expected from our 'snapshot' sampling of a community with potentially high-frequency internal predator-prey cycles and the relatively low sample number in some cases. Thus no distinct seasonal signal was observed (Fig. 7a,b); nor were ratios clearly related to chlorophyll concentration (Fig. 7c,d). Median biomass ratios centered around 0.3, although the east region exhibited lower median and maximum ratios throughout 2011, as well as in summer 2013. Low MZ:P ratios were all clearly related to lows in microzooplankton biomass (Fig. 2a, b), while high values (≥ 0.5) were confined to chlorophyll concentrations < 2 µg liter^{-1}. Note that the ability of MZ:P biomass ratios to represent trophic transfer efficiencies (the ratio of microzooplankton production to phytoplankton production) depends on equivalence of production:biomass ratios for each of

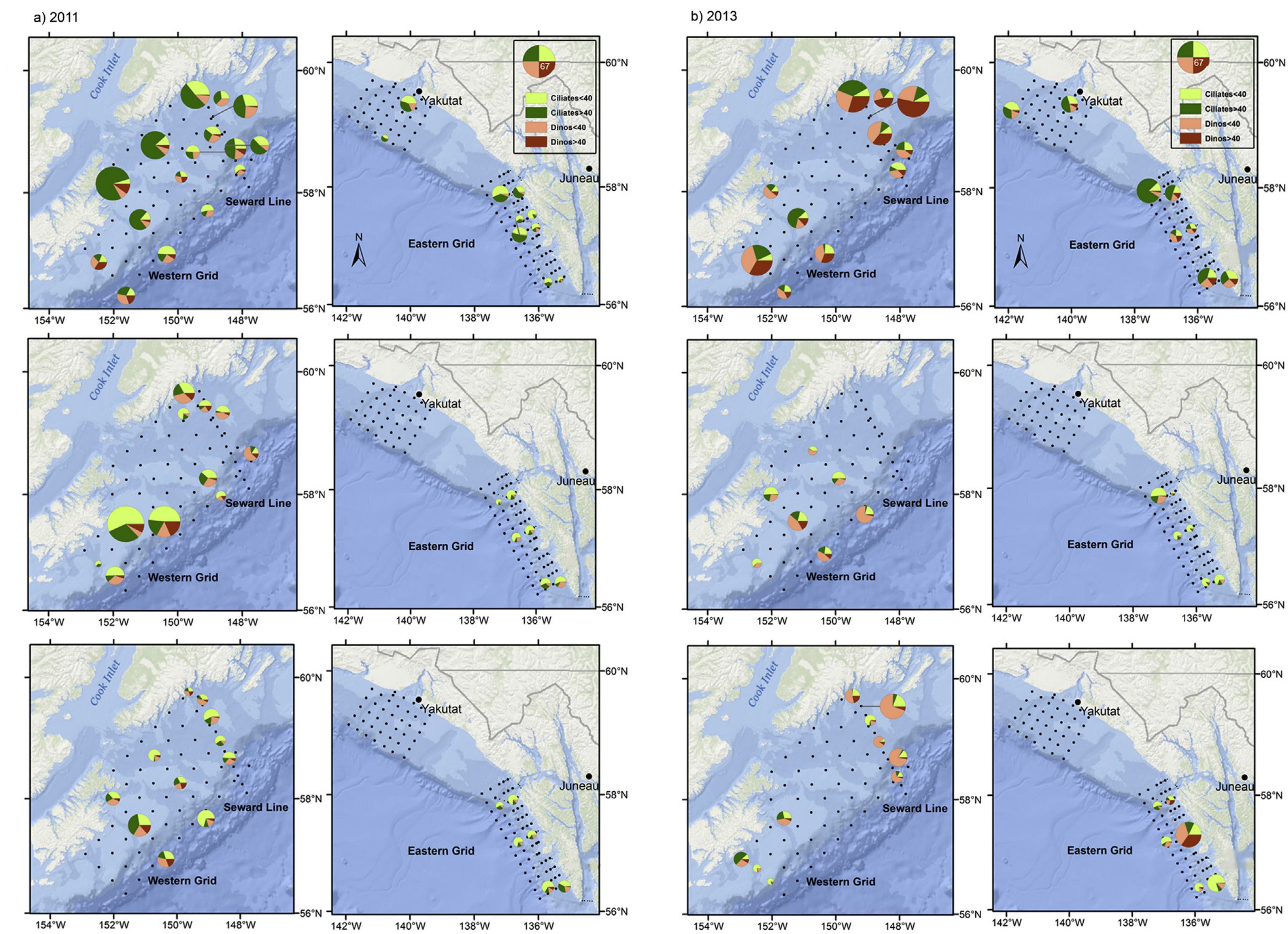

Fig. 3. Maps of microzooplankton biomass distribution in a) 2011 and b) 2013. Left panels show western grid; right panels show eastern grid. Upper panels are spring, middle are summer, and lower are fall. Color/shading indicates taxonomic/size composition of community, as indicated in legend at upper right. Circle areas are proportional to total microzooplankton biomass (area of circle in legend is equivalent to 67 μg C liter^{-1}). Symbols for Seward Line are sometimes offset from actual sampling location to avoid overlap.

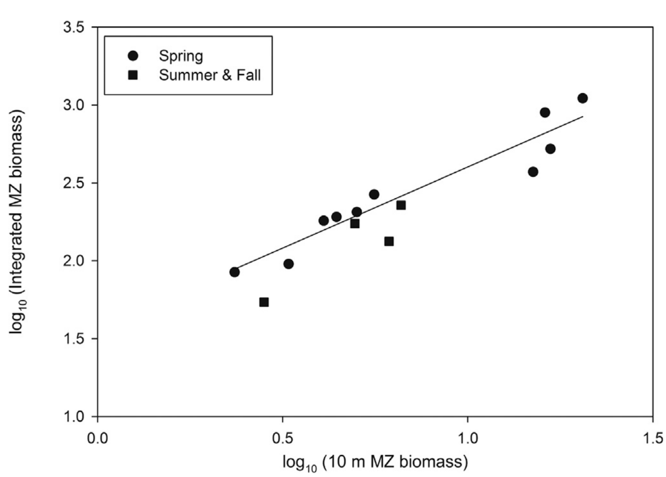

Fig. 4. Log-log relationship between microzooplankton biomass at 10 m depth (MZ10; μg C liter^{-1}) and integrated (0–50 m) microzooplankton biomass (MZint; mg C m^{-2}) for 14 vertical profiles collected during 2011. Circles = spring; squares = summer and fall. $\log_{10}$(MZint) = 1.13($\log_{10}$MZ10) + 1.44; r^2 = 0.87.

the two trophic levels (MZ and P) in the relationship. There are few (if any) data with which to evaluate this not-unreasonable assumption.

Variation in the microzooplankton community was strongly predicted by PC1 (Fig. 8). The uniformly positive coefficients (Table 4) indicate that a single factor – microzooplankton biomass - was largely responsible for the partitioning observed along that axis. Groups contributing most strongly to PC1 were the largest oligotrich ciliates as well as the largest dinoflagellates in the *Gyrodinium/Gymnodinium* complex. Thus high biomass microzooplankton assemblages were strongly associated with increases in the largest microzooplankton. PC1 was also significantly correlated with Chl (r = 0.566), but not with other environmental measures. Separation of communities along PC2 was clearly related to ciliate versus dinoflagellate dominance of total biomass (Fig. 8A; Table 4). Curiously, the tintinnid ciliates grouped with the dinoflagellates in terms of separation along PC2. In general, the major separation of communities according to PCA was by region (Fig. 8C). Microzooplankton assemblages from the east tended to cluster at low values of PC1 (lower biomass) and at higher values of PC2 (ciliate dominance), while assemblages from the west were found throughout the analysis space. In contrast to this regional separation, we saw little separation of communities by year or by season (Fig. 8A, B).

Results of the BIO-ENV analysis indicated that, of the suite of environmental variables considered (temperature, salinity,

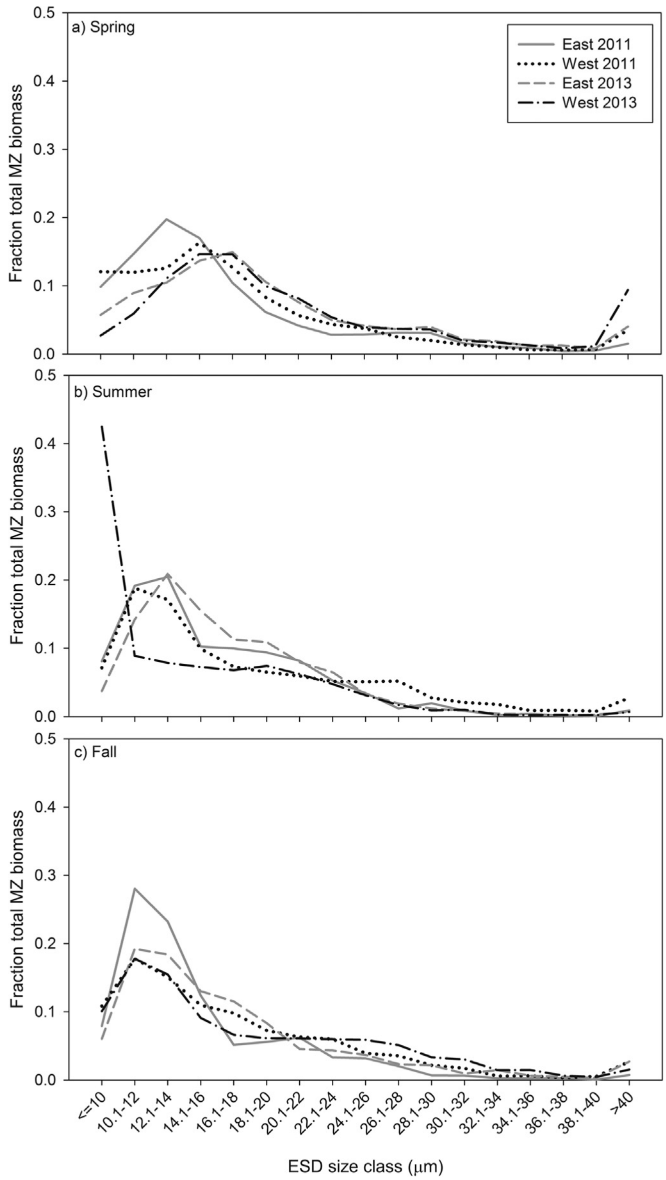

Fig. 5. Average size frequency distributions of microzooplankton Equivalent Spherical Diameter (ESD, µm) in 2011 and 2013 for a) spring; b) summer; and c) fall in east and west sampling regions of the coastal Gulf of Alaska. Note that ESD does not represent actual maximum dimensions of most cells, as most were not spherical.

macronutrients, Chl), none was a strong predictor of microzooplankton community structure, either singly or in combination. The highest Spearman rank correlation between biotic and environmental patterns was only a relatively weak 0.227 (for the combination of temperature, ammonium, and Chl).

4. Discussion

4.1. East-west contrasts

Of the three 'axes of variability' explored in this study – interannual, seasonal and regional – the largest contrasts were associated with region. Microzooplankton communities in the eastern CGOA consistently tended toward a lower biomass and a higher proportion of ciliates than communities in the west; eastern biomass levels were also conspicuously low relative to historical estimates from the western CGOA (Table 5). In many seasons/years the east also showed lower MZ:P ratios than the west. Indeed, the only microzooplankton community measure that did not show a clear regional difference was size composition. Based on PCA, no communities separated completely along any of our axes of variability, indicating substantial basin-scale

Table 3
Comparison of < 20 µm heterotrophic flagellate versus microzooplankton biomass (µg C liter^{-1}) during spring in the eastern coastal Gulf of Alaska. All samples from 10 m depth. See Fig. 1 for station locations. H = heterotrophic; dino = dinoflagellate; flag = flagellate; nd = not detected.

		< 20 µm flagellates		Microzooplankton			
Date	Station	Hdino	Hflag	Dino	Ciliate	Total	% < 20 flag
2011							
5–5	SEA5	1.1	0.3	0.4	1.9	3.7	37
5–5	SEA20	1.9	2.3	0.3	4.1	8.6	49
5–8	SEK5	8.5	2.8	0.7	8.3	20.3	56
5–8	SEK20	5.1	8.5	1.1	16.8	31.5	43
5–11	YBC50	2.8	3.7	0.2	3.1	9.8	66
5–11	YBC10	4.3	3.2	3.1	13.6	24.3	31
5–18	SEG5	nd	8.9	1.2	3.8	13.9	64
2013							
4–11	SEG5	1.9	5.5	3.4	3.6	14.4	51
4–14	SEA5	0.3	1.1	7.5	11.9	20.8	7
4–15	SEA20	0.3	3.7	9.2	14.8	27.9	14
4–19	YBC10	2.2	1.8	4.0	13.7	21.8	18
4–21	YBG50	3.1	0.4	4.4	13.8	21.8	16

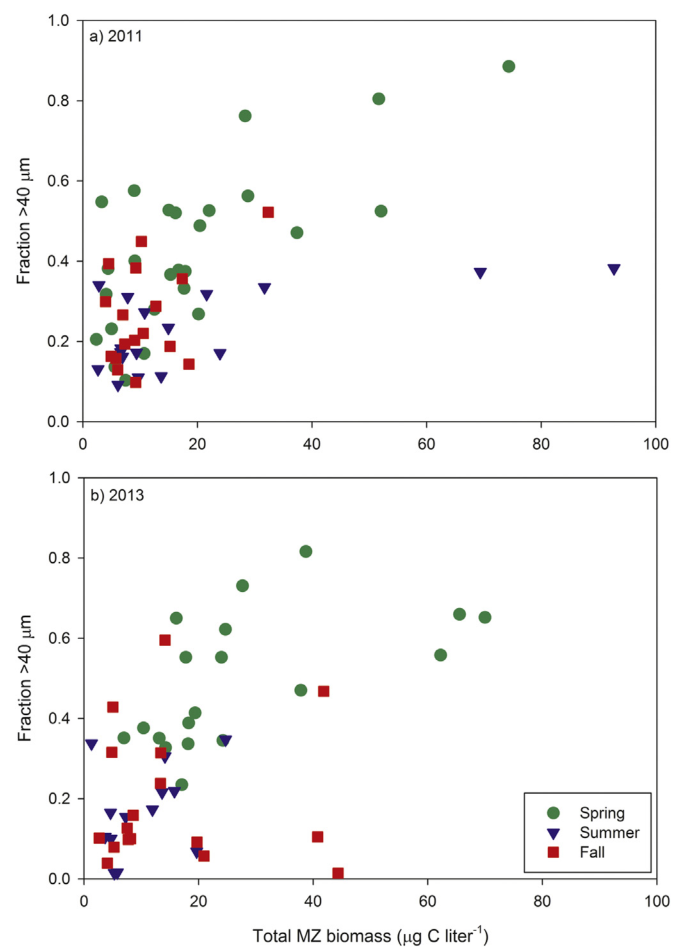

Fig. 6. Relationship between total microzooplankton biomass at 10 m depth (µg C liter^{-1}) and the fraction of the total biomass found in microzooplankton cells > 40 µm in longest dimension, for a) 2011 and b) 2013. Symbols/colors show different sampling seasons.

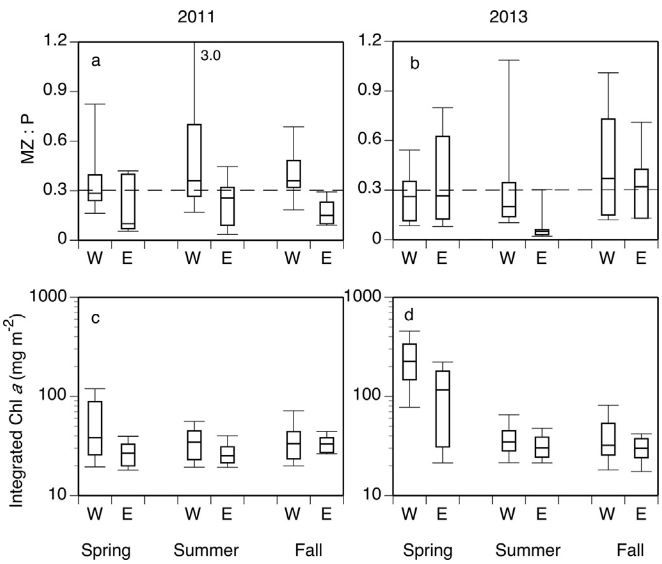

Fig. 7. Box plots of microzooplankton: phytoplankton carbon biomass ratios (a, b) and integrated (0–50 m) water column chlorophyll *a* (c, d) for western and eastern regions during 3 seasons for 2011 (left panels) and 2013 (right panels). Data in a and b from 10 m samples; see methods for details. Top, bottom and line through center of boxes denote 75th percentile, median (50th percentile) and 25th percentile of the data, respectively. Whiskers extend from the 10th percentile to the 90th. Dashed horizontal lines in c and d indicate ratio of 0.3.

coherence at least at the coarse taxonomic/size categorization scale employed here. However, grouping of samples by region was stronger than grouping by either year or season (Fig. 8).

The geomorphology of the eastern shelf probably predisposes this region to lower primary productivity than the west, which could underlie the east-west contrasts we observed in the microzooplankton community. The narrow eastern shelf (Fig. 1), combined with rugged topography, promotes cross-shelf exchange between coastal and oceanic waters through a variety of mechanisms including gap winds, tides, and mesoscale eddies (Henson and Thomas, 2008; Ladd, 2007; Ladd and Cheng, 2016; Stabeno et al., 2016). While cross-shelf transport and mixing processes are thought to locally enhance primary production, in the aggregate this narrow shelf appears to have a more oceanic character than the broader shelf to the west due to substantial on-shelf transport of oceanic water and off-shelf transport of coastal water (Stabeno et al., 2016).

Evidence for lower productivity in the east is seen in satellite ocean color data: eastern near-surface chlorophyll concentrations averaged 30% lower on an annual basis, and 40% lower during spring and fall blooms, than those in the western region (1998–2011 period; Waite and Mueter, 2013). Our extensive data set of in situ (extracted) Chl measurements, encompassing nearly 500 stations, shows a similar western enhancement of chlorophyll during spring and summer (note that, at least during spring, extracted Chl is a robust proxy for primary productivity in the CGOA; Strom et al., 2016, their Table 1). However, conclusions from the satellite versus in situ data differ for the fall season, when in situ data show approximately equal median Chl (though higher western maxima) for the two regions. An in-depth comparison of satellite-based versus in situ Chl estimates will be required to reconcile these differences, which are already known to be problematic in the CGOA (Waite and Mueter, 2013).

The consistently higher proportion of ciliates in the east (discussed below), as well as the lower MZ:P ratios, strongly suggest east-west differences in the composition as well as the amount of primary production in the two regions, perhaps in combination with regional differences in top-down processes such as mesozooplankton grazing (Hopcroft and Clarke, personal communication). Reduced suitability of prey (i.e. cells less efficiently captured, or less nutritious once ingested)

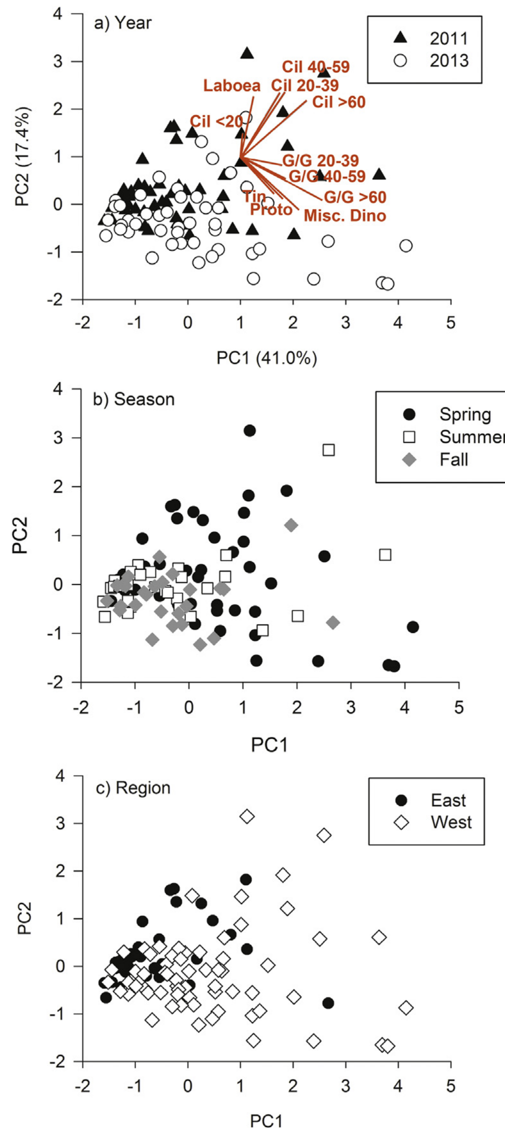

Fig. 8. Principal components analysis (PCA) ordination of microzooplankton data with symbols coded by a) year; b) season; and c) region. Arrows in a) show taxon/size class loadings, with axis labels showing % of total variance explained by PC1 and PC2. See Table 4 for regression coefficients and taxon/size class definitions.

could give rise to lower microzooplankton growth efficiencies, leading to lower MZ:P biomass ratios. This would be consistent with a more oceanic character on this shelf: phytoplankton in nearby oceanic subarctic waters tend to be very small (i.e. $\leq$ 5 µm, or ultraplanktonic; Booth et al., 1993). This leads to inefficient capture by most larger ciliates and dinoflagellates (Hansen et al., 1994), and likely adds at least one trophic level (e.g. heterotrophic nanoflagellates) to the food web. As well, these oceanic communities can have a high proportion of < 2 µm cyanobacteria (*Synechococcus*) that, even when ingested, appear to be of low nutritional value for many microzooplankton (Apple et al., 2011; Christaki et al., 1999; Verity and Villareal, 1986). We observed exactly these features (high proportion of ultraphytoplankton, including *Synechocccus*) in the low chlorophyll spring community of 2011 on the eastern shelf (Strom et al., 2016). Similarly, higher predation by mesozooplankton in the east, especially if preferentially affecting microzooplankton over phytoplankton (e.g. Gifford, 1993; Dagg et al., 2009; Liu et al., 2005), could also contribute to lower eastern MZ:P ratios.

Further south along the west coast of the continental U.S., primary

Table 4
Properties of principal components derived from PCA of microzooplankton data. General properties of the analysis are followed by coefficients (eigenvectors) for each of the 11 size class/taxonomic variables. Coefficients with greatest predictive power (values > 0.4 or < -0.4) are highlighted in **bold** for the first 3 principal components. Dinoflagellates include Gyro/Gymno (= dinoflagellates in the *Gyrodinium* spp./*Gymnodinium* spp. complex), Proto-like (= *Protoperidinium* and related thecate genera), and miscellaneous. Ciliates include oligotrichs, tintinnids, and the chloroplast-retaining species *Laboea strobila*. Size class designations refer to largest cell dimension.

	PC1	PC2	PC3
Eigenvalue	1.63	0.691	0.551
% variation	41	17.4	13.9
Cumulative % variation	41	58.4	72.3
Variable:			
Oligotrich Ciliate < 20 µm	0.009	0.155	− 0.267
Oligotrich Ciliate 20–39 µm	0.245	**0.418**	− 0.275
Oligotrich Ciliate 40–59 µm	0.296	**0.449**	− 0.207
Oligotrich Ciliate > 60 µm	**0.420**	0.367	**0.622**
Laboea strobila	0.079	0.393	0.012
Tintinnids	0.218	− 0.218	− 0.076
Gyro/Gymno 20–39 µm	0.261	− 0.043	− **0.597**
Gyro/Gymno 40–59 µm	0.279	− 0.132	− 0.111
Gyro/Gymno > 60 µm	**0.520**	− 0.266	0.129
Proto-like	0.262	− 0.253	0.151
Misc. Dinoflagellate	0.369	− 0.329	− 0.094

Table 5
Comparison of seasonal microzooplankton biomass estimates (µg C liter^{-1}) from the coastal Gulf of Alaska (CGOA) and other shelf seas at a similar latitude. The Seward Line is included in the western region of the present study (Fig. 1). Where vertical profiles were reported, values are means of estimates from the upper water column (most sampling depths ≤ 15 m); all studies collected, preserved and analyzed samples with comparable methods. In some instances data were extracted from published figures using DataThief III. Weighted averages were computed in cases where studies reported means from separate zones or time periods. nr = not reported.

Year	Season			Region	n	Source
	Spring	Summer	Fall			
Coastal Gulf of Alaska						
1990	47			Shelikof Strait	3	Howell-Kubler et al. (1996)
1998	13			Seward Line	3	Strom et al. (2001)
1999	16			Seward Line	4	Strom et al. (2001)
2001	26	29		Seward Line	19,10	Strom et al. (2007)
2011	8	7	6	Eastern CGOA	6–10	This study
	26	27	13	Western CGOA	11–16	
2013	19	6	14	Eastern CGOA	6–8	This study
	34	12	16	Western CGOA	7–11	
Bering Sea						
1999		57		SE Bering	13	Olson and Strom (2002)
2004		30		SE Bering	19	Strom and Fredrickson (2008)
2008–10	20			Eastern Bering	79	Sherr et al. (2013)
2008–10		20		Eastern Bering	202	Stoecker et al. (2014)
Eastern North Atlantic						
1987–89	13			Irish Sea	nr	Edwards and Burkill (1995)
2007–09	41	122	62	SE North Sea	11–22	Gunther et al. (2012)
2009	23			English Channel	9	Grattepanche et al. (2011)

productivity is strongly and positively correlated with shelf width (Chase et al., 2007), a relationship attributed to storage of reactive iron – and possibly dissolved iron binding ligands - in shelf sediments (Bruland et al., 2001; Bundy et al., 2015; Johnson et al., 1999). Iron is the key limiting nutrient for phytoplankton in the high nitrate-low chlorophyll waters of the open Gulf of Alaska (Boyd et al., 2004). Iron limitation of phytoplankton production on the northeastern Pacific shelf has been demonstrated by iron addition experiments along the California coast (Firme et al., 2003; Hutchins et al., 1998), and by molecular techniques in coastal British Columbia (Chappell et al., 2015). Given hydrological differences, the relationships among iron inputs, storage, and utilization in the CGOA are likely to contrast with those further south. However, a relationship between shelf width and the storage and delivery of terrestrially derived iron may contribute to lower production in the east versus west CGOA study regions, as it does to production gradients along the coastline from California to British Columbia.

4.2. Microzooplankton community composition

A striking and unexpected feature of our data set was the predominance of ciliates, which dominated microzooplankton biomass throughout the coastal Gulf in 2011, and throughout the eastern region in 2013. In the east, the median ciliate:dinoflagellate biomass ratio was always > 2, and was > 5 throughout 2011, regardless of season. This very high proportion of ciliates contrasts strongly with data from the Bering Sea, where dinoflagellates typically constitute half or more of the microzooplankton biomass in both spring and summer (Stoecker et al., 2014; their Table 3). Based on the east-west differences discussed above, we speculate that ciliate dominance in the CGOA is related to lower productivity environments, while dinoflagellates are associated with times/locations of higher production. For example, in the spring Bering Sea, a positive relationship between Chl and the proportion of dinoflagellates was observed (Sherr et al., 2013). However, we saw no such relationship in our data nor, more broadly, between microzooplankton community composition and any measured environmental property. We attribute this to the relatively coarse nature of our taxonomic analysis, combined with a heterogeneous environment comprising a dynamic mosaic of environmental conditions.

Stoecker et al. (2014), in their examination of the summer Bering Sea microzooplankton community, found that a large proportion of the ciliates belonged to chloroplast-retaining species, including *Laboea strobila* and *Strombidium* spp. We did not observe high abundances of *L. strobila*, but they were more common in 2011 than 2013, and within the more productive 2013, were more commonly observed in the east than in the west. In addition to *L. strobila*, ciliates closely resembling described chloroplast-retaining *Strombidium* spp. comprised a high percentage of the oligotrich community in our samples. We hypothesize that many of the larger oligotrichs in the CGOA are chloroplast-retaining species, as seen in the (hydrographically connected) Bering Sea. These ciliates, which sequester functional chloroplasts from their phytoplankton prey, are thought to use the photosynthate to improve survival in times of prey scarcity. This process also repackages phytoplankton biomass and associated production into a larger particle (the ciliate) that is more efficiently captured by mesozooplankton predators (see Section 4.4, below). In contrast, the smallest ciliates, which may or may not be chloroplast-retaining, occupy a different niche. Due to their reduced size and high relative clearance rates, these microzooplankters can do well even when prey are both dilute and ultraplanktonic (e.g. Berninger and Wickham, 2005; Ferrier-Pages and Gattuso, 1998). Thus the smallest and largest ciliates may represent different adaptations to conditions of prey scarcity, giving rise to the observed broad-scale association between ciliate dominance and times/places of lower productivity in the CGOA. This relationship is supported by 2001 data from the CGOA showing a cross-shelf gradient in microzooplankton community composition, with > 60% ciliates found only on the outer shelf or in pre-spring bloom conditions (Strom et al., 2007; their Fig. 6B).

The largest dinoflagellates in the coastal GOA ecosystem are not mixotrophic; rather, they are strict heterotrophs belonging to either the *Gyrodinium/Gymnodinium* complex, or to the genus *Protoperidinium* and closely related thecate pallium-feeders. Using diverse feeding mechanisms, species in both of these groups can grow rapidly on large diatoms (Hansen, 1992; Jacobson and Anderson, 1993), and collectively are thought to be the major grazers of diatoms in the coastal ocean (Sherr and Sherr, 2007). In one well-documented regional example, the iron fertilization-induced western subarctic bloom of the chain diatom *Chaetoceros debilis* was largely terminated by *Gyrodinium* spp. grazing pressure (Saito et al., 2006). Similarly, Strom et al. (2007) found that grazing by microzooplankton was equivalent to 41% of growth rates in the diatom size fraction during spring diatom blooms along the Seward Line, with large dinoflagellates as major contributors to microzooplankton biomass in most instances.

We observed a significant correlation between PC1 and Chl, with PC1 related most strongly to the biomass of the largest ciliates and dinoflagellates. The analysis above suggests the underpinnings of this correlation are complex. The largest ciliates are likely chloroplast-retaining and thus mixotrophs, contributing directly to Chl (and photosynthesis) in the > 20 µm size fraction while actively consuming smaller cells. In contrast, the largest dinoflagellates are heterotrophs whose abundance increases in association with diatoms, the dominant phytoplankton group during high-Chl spring blooms in the CGOA.

4.3. Seasonal and interannual contrasts in microzooplankton

The two years studied here represent a strong contrast in terms of the timing and intensity of the spring bloom. Spring 2011 showed little or no spring bloom, as evident from satellite imagery and field sampling of Chl (Stabeno et al., 2016; Waite and Mueter, 2013). Bloom depression was particularly severe in the eastern coastal Gulf, where we observed a sparse phytoplankton community of mostly ultraplanktonic cells with reduced photosynthetic capacity and low growth rates in comparison to spring 2013 (Strom et al., 2016).

Features of the microzooplankton closely mirror those seen in the spring 2011 phytoplankton community: reduced biomass, most strongly in the east, along with a shift in emphasis to the smallest cells in the ecosystem. Accompanying this was a clear reduction in spring MZ:P biomass ratios, also in the eastern region (median 0.10 versus 0.27 for 2011 and 2013, respectively). These interannual differences were not seen in summer or fall. In contrast, interannual differences in community composition showed greater persistence, with 2011 more ciliate-dominated than 2013 through the summer and fall. As well, the smallest heterotrophic flagellates were greater contributors to total protist grazer biomass in the spring of 2011 than in spring of 2013 (data not available for summer or fall). Thus the conditions in spring 2011 seem to have driven the entire CGOA toward microzooplankton community states more commonly seen in the eastern region, as discussed above. Although we do not yet understand the reasons for the persistence of ciliate dominance throughout 2011, the contrast with 2013 does suggest that underlying primary production and/or mesozooplankton predation regimes differed to some degree throughout the entire spring-summer-fall period.

Seasonal differences are best assessed from the 2013 data; the lack of a 2011 spring bloom dampened seasonal cycles in that year. Data for 2013 show a strong spring maximum in microzooplankton biomass and in the proportion of large microzooplankton cells. These two properties were inter-related, in that, as for Chl (Stabeno et al., 2016), addition of spring microzooplankton biomass tended to be due to the addition of large-celled ciliates and dinoflagellates. Lower (2013) median and maximum biomass in fall than in spring reflects the lower magnitude of the fall phytoplankton bloom (Brickley and Thomas, 2004; Childers et al., 2005; Waite and Mueter, 2013). Further, there was no fall increase in microzooplankton cell size relative to summer. Summer appears to represent a seasonal low in microzooplankton biomass. Past data sometimes indicate higher summer means (Table 5), but these are heavily influenced by sampling in high Chl ‘hot spots’ such as the ACC (station GAK-1 on the Seward Line in 2001) and the shallow banks southeast of Kodiak Island (see for example Fig. 5 in Waite and Mueter, 2013).

In contrast to biomass, we saw no seasonal cycle in gross taxonomic composition (ciliates versus dinoflagellates), nor did PCA indicate strong separation of communities by season even when applied to 2013 data alone, indicating considerable overlap in gross community composition across all seasons. However, as for biomass, there was a suggestion that spring and fall MZ:P biomass ratios were higher than those in summer. Overall, assuming 2013 represents a more typical seasonal cycle, spring and fall bloom periods appear to be times of higher microzooplankton biomass and trophic transfer efficiency, but with distinct differences (smaller microzooplankton cells, lower median microzooplankton biomass) in fall relative to spring.

Cruise timing issues could have played a role in our perception of regional and interannual differences. In a given season, cruises to the east generally preceded cruises to the west (Table 1). However, this timing difference is not clearly related to the overarching east-west dichotomies in the data that were discussed in Section 4.1. For example, although western biomass estimates were generally higher than in the east, the later timing of fall cruises to the west (late September – early October) seems likely to have under- rather than over-represented the microzooplankton response to the fall production peak in those waters. Similarly, the offset in timing of the spring cruises in the east (almost a month earlier in 2013 than in 2011) could have influenced our conclusions about interannual contrasts. However, high macronutrient concentrations during both cruises indicate we captured both springs at the early bloom stage, the major contrast being that the high Chl seen in April 2013 apparently never developed in spring 2011. In summary, the regional and interannual contrasts described here for microzooplankton appear to be robust features of the ecosystem response rather than artifacts of cruise timing.

4.4. Microzooplankton relationships to higher trophic levels

Microzooplankton are known to be important prey for crustacean zooplankton, mucous net feeders such as salps and pteropods, and larval fish, all key components of the CGOA planktonic food web (Montagnes et al., 2010; Stoecker, 2013; Stoecker and Capuzzo, 1990). Variation in abundance, size, and taxonomic composition of microzooplankton will strongly influence production at these higher trophic levels. Prey abundance influences feeding and reproduction rates for essentially all zooplankton, including CGOA species (e.g. Frost et al., 1983; Jonasdottir, 1989; Pinchuk and Hopcroft, 2007). Large microzooplankton cells are the most readily captured and ingested by higher trophic level consumers such as large copepods, euphausiids, and larval fish (Dagg et al., 2009; de Figueiredo et al., 2007; Du and Peterson, 2014); ciliates and sometimes dinoflagellates appear to be preferred over phytoplankton (Gifford, 1993; Dagg et al., 2009; Liu et al., 2005), especially in low-chlorophyll waters where they can constitute a substantial fraction of the copepod diet (reviewed by Saiz and Calbet, 2011). Taken together, these features of trophic coupling indicate that times and places of low microzooplankton biomass, generally found in conjunction with small microzooplankton cells, are challenging feeding environments for many mesozooplankton. Examples in this study include much of the eastern shelf, the summer season, and years such as 2011 with anomalously low spring production. Our data show the highest availability of large microzooplankton during the high-chlorophyll spring of 2013. However, the strategy of chloroplast sequestration by large oligotrich ciliates could also be key to making primary production available to higher consumers at less productive times.

Mucous net feeders, including salps, larvaceans and pteropods, constitute an exception to the paradigm described above. Able to feed upon even the smallest planktonic prey with high efficiency, these consumers have the potential 'short-circuit' multi-level food webs by linking ultraplankton production directly to vertebrate trophic levels and to vertical export (Fortier et al., 1994). In 2011, high abundances of salps were observed in both spring (*Salpa aspera*, especially in the eastern region) and summer (*Cyclosalpa bakeri*; Li et al., 2016). Presence of these mucous net feeders during this low-chlorophyll, low-microzooplankton year could have enhanced trophic transfer and/or led to anomalously high vertical export. Calculations show that *S. aspera* grazing could also have exerted moderate top-down control of phytoplankton accumulation, thus contributing to the lack of a spring bloom in that year at least in the eastern region (Li et al., 2016).

4.5. Summary

We have previously shown that ~all small phytoplankton production and nearly half of large phytoplankton production is consumed by microzooplankton in the CGOA (Strom et al., 2007). Therefore, properties of the microzooplankton community in those waters – taxonomic and size composition, abundance and biomass – as well as the phyto-microzooplankton trophic transfer efficiency, are of critical importance for determining access by higher trophic levels to the episodically rich production at the base of the CGOA food web. This study demonstrates substantial variability in microzooplankton community properties across temporal and regional gradients. Major findings:

1. We observed strong regional (east versus west) contrasts in the biomass and taxonomic composition of the microzooplankton community. The eastern region exhibited generally lower microzooplankton biomass and a greater proportion of ciliates than the west, even in the face of basin-wide seasonal and interannual contrasts. These differences were almost certainly a consequence of the lower productivity environment in the east, which is in turn related to the narrower shelf and vigorous cross-shelf exchange processes there.
2. This study encompassed two strongly contrasting years: 2011, with a minimal spring bloom, and 2013, with an early, strong spring bloom. This contrast was reflected in the spring microzooplankton biomass (lower in 2011) and in the greater representation of ciliates throughout 2011. Ciliate dominance could reflect different adaptations of both the smallest and largest ciliates to lower productivity conditions.
3. MZ:P biomass ratios varied widely over time and space. These ratios suggest that lower productivity regions (east) and seasons (summer) are also locations/times of reduced trophic transfer efficiency from phytoplankton to ciliates and dinoflagellates. Ciliates and dinoflagellates can be preferred prey of mesozooplankton, including dominant CGOA copepod species. Thus multiple mechanisms conspire to reduce the flow of matter and energy to higher trophic levels during low productivity periods in the CGOA.

Acknowledgements

We thank the captains and crew of all the GOA-IERP research vessels, as well as K. Brown, A. Kolb, S. McKeever, C. Mordy, M. Ostendorf, A. Skorupa, and E. Wisegarver for their assistance in collecting microzooplankton samples. Funding for this study was provided by the North Pacific Research Board as part of the GOA-IERP program. This is NPRB publication #675 and GOA-IERP publication #31.

Appendix A. Supporting information

Supplementary data associated with this article can be found in the online version at https://doi.org/10.1016/j.dsr2.2018.07.012.

References

Apple, J.K., Strom, S.L., Palenik, B., Brahamsha, B., 2011. Variability in protist grazing and growth on different marine *Synechococcus* isolates. Appl. Environ. Microbiol. 77, 3074–3084.
Aydin, K.Y., McFarlane, G.A., King, J.R., Megrey, B.A., Myers, K.W., 2005. Linking oceanic food webs to coastal production and growth rates of Pacific salmon (*Oncorhynchus* spp.), using models on three scales. Deep-Sea Res. II 52, 757–780.
Berninger, U.-G., Wickham, S.A., 2005. Response of the microbial food web to manipulation of nutrients and grazers in the oligotrophic Gulf of Aqaba and northern Red Sea. Mar. Biol. 147, 1017–1032.
Booth, B.C., Lewin, J., Postel, J.R., 1993. Temporal variation in the structure of autotrophic and heterotrophic communities in the subarctic Pacific. Prog. Oceanogr. 32, 57–99.
Boyd, P.W., Law, C.S., Wong, C.S., Nojiri, Y., Tsuda, A., Levasseur, M., Takeda, S., Rivkin, R., Harrison, P.J., Strzepek, R., Gower, J., McKay, R.M., Abraham, E., Arychuk, M., Barwell-Clarke, J., Crawford, W., Crawford, D., Hale, M., Harada, K., Johnson, K., Kiyosawa, H., Kudo, I., Marchetti, A., Miller, W., Needoba, J., Nishioka, J., Ogawa, H., Page, J., Robert, M., Saito, H., Sastri, A., Sherry, N., Soutar, T., Sutherland, N., Taira, Y., Whitney, F., Wong, S.E., Yoshimura, T., 2004. The decline and fate of an iron-induced subarctic phytoplankton bloom. Nature 428, 549–553.
Brickley, P.J., Thomas, A.C., 2004. Satellite-measured seasonal and interannual chlorophyll variability in the northeast Pacific and coastal Gulf of Alaska. Deep-Sea Res. 51, 229–245.
Bruland, K.W., Rue, E.L., Smith, G.J., 2001. Iron and macronutrients in California coastal upwelling regimes: implications for diatom blooms. Limnol. Oceanogr. 46, 1661–1674.
Bundy, R.M., Abdulla, H.A.N., Hatcher, P.G., Biller, D.V., Buck, K.N., Barbeau, K.A., 2015. Iron-binding ligands and humic substances in the San Francisco Bay estuary and estuarine-influenced shelf regions of coastal California. Mar. Chem. 173, 183–194.
Calbet, A., Landry, M.R., 2004. Phytoplankton growth, microzooplankton grazing, and carbon cycling in marine systems. Limnol. Oceanogr. 49, 51–57.
Chappell, P.D., Whitney, L.P., Wallace, J.R., Darer, A.I., Jean-Charles, S., Jenkins, B.D., 2015. Genetic indicators of iron limitation in wild populations of *Thalassiosira oceanica* from the northeast Pacific Ocean. ISME J. 9, 592–602.
Chase, Z., Strutton, P.G., Hales, B., 2007. Iron links river runoff and shelf width to phytoplankton biomass along the U.S. West Coast. Geophys. Res. Lett. 34, L04607 (doi:04610.01029/02006GL028069).
Childers, A.R., Whitledge, T.E., Stockwell, D.A., 2005. Seasonal and interannual variability in the distribution of nutrients and chlorophyll a across the Gulf of Alaska shelf: 1998–2000. Deep-Sea Res. ll 52, 193–216.
Christaki, U., Jacquet, S., Dolan, J.R., Vaulot, D., Rassoulzadegan, F., 1999. Growth and grazing on *Prochlorococcus* and *Synechococcus* by two marine ciliates. Limnol. Oceanogr. 44, 52–61.
Coyle, K.O., Cheng, W., Hinckley, S.L., Lessard, E.J., Whitledge, T.E., Hermann, A.J., Hedstrom, K., 2012. Model and field observations of effects of circulation on the timing and magnitude of nitrate utilization and production on the northern Gulf of Alaska shelf. Prog. Oceanogr. 103, 16–41.
Coyle, K.O., Gibson, G.A., Hedstrom, K., Hermann, A.J., Hopcroft, R.R., 2013. Zooplankton biomass, advection and production on the northern Gulf of Alaska shelf from simulations and field observations. J. Mar. Syst. 128, 185–207.
Coyle, K.O., Pinchuk, A.I., 2005. Cross-shelf distribuiton of zooplankton relative to water masses on the northern Gulf of Alaska shelf. Deep-Sea Res. II 52, 217–245.
Dagg, M., Strom, S., Liu, H., 2009. High feeding rates on large particles by *Neocalanus flemingeri* and *N. plumchrus*, and consequences for phytoplankton community structure in the subarctic Pacific Ocean. Deep-Sea Res. I 56, 716–726.
de Figueiredo, G.M., Nash, R.D.M., Montagnes, D.J.S., 2007. Do protozoa contribute significantly to the diet of larval fish in the Irish Sea? J. Mar. Biol. Assoc. U.K. 87, 843–850.
Du, X., Peterson, W., 2014. Feeding rates and selectivity of adult *Euphausia pacifica* on natural particle assemblages in the coastal upwelling zone off Oregon, USA, 2010. J. Plankton Res. 36, 1031–1046.
Edwards, E.S., Burkill, P.H., 1995. Abundance, biomass and distribution of microzooplankton in the Irish Sea. J. Plankton Res. 17, 771–782.
Ferrier-Pages, C., Gattuso, J.-P., 1998. Biomass, production and grazing rates of pico- and nanoplankton in coral reef waters (Miyako Island, Japan). Microb. Ecol. 35, 46–57.
Fiechter, J., Moore, A.M., 2009. Interannual spring bloom variability and Ekman pumping in the coastal Gulf of Alaska. J. Geophys. Res. 114 (C06004, doi:06010.01029/02008JC005140).
Fiechter, J., Moore, A.M., Edwards, C.A., Bruland, K.W., Di Lorenzo, E., Lewis, C.V.W., Powell, T.M., Curchister, E.N., Hedstrom, K., 2009. Modeling iron limitation of primary production in the coastal Gulf of Alaska. Deep-Sea Res. II 56, 2503–2519.
Firme, G.F., Rue, E.L., Weeks, D.A., Bruland, K.W., Hutchins, D.A., 2003. Spatial and temporal variability in phytoplankton iron limitation along the California coast and consequences for Si, N, and C biogeochemistry. Glob. Biogeochem. Cycles 17. https://doi.org/10.1029/2001GB001824.
Fortier, L., Le Fevre, J., Legendre, L., 1994. Export of biogenic carbon to fish and to the deep ocean: the role of large planktonic microphages. J. Plankton Res. 16, 809–839.
Frost, B.W., Landry, M.R., Hassett, R.P., 1983. Feeding behavior of large calanoid copepods *Neocalanus cristatus* and *N. plumchrus* from the subarctic Pacific Ocean. Deep-Sea Res. 30, 1–13.
Gaichas, S.K., Aydin, K.Y., Francis, R.C., 2010. Using food web model results to inform stock assessment estimates of mortality and production for ecosystem-based fisheries management. Can. J. Fish. Aquat. Sci. 67, 1490–1506.
Gifford, D.J., 1993. Protozoa in the diets of *Neocalanus* spp. in the oceanic subarctic

Pacific Ocean. Prog. Oceanogr. 32, 223–237.
Grattepanche, J.-D., Vincent, D., Breton, E., Christaki, U., 2011. Microzooplankton herbivory during the diatom-*Phaeocystis* spring succession in the eastern English Channel. J. Exp. Mar. Biol. Ecol. 404, 87–97.
Günther, M., Löder, J., Kraberg, A.C., Aberle, N., Peters, S., Wiltshire, K.H., 2012. Dinoflagellates and ciliates at Helgoland Roads, North Sea. Helgol. Mar. Res. 66, 11–23.
Hansen, B., Bjornsen, P.K., Hansen, P.J., 1994. The size ratio between planktonic predators and their prey. Limnol. Oceanogr. 39, 395–403.
Hansen, P.J., 1992. Prey size selection, feeding rates and growth dynamics of heterotrophic dinoflagellates with special emphasis on *Gyrodinium spirale*. Mar. Biol. 114, 327–334.
Henson, S.A., Thomas, A.C., 2008. A census of oceanic anticyclonic eddies in the Gulf of Alaska. Deep-Sea Res. I 55, 163–176.
Hinckley, S.L., Coyle, K.O., GIbson, G., Hermann, A.J., Dobbins, E.L., 2009. A biophysical NPZ model with iron for the Gulf of Alaska: reproducing the differences between an oceanic HNLC ecosystem and a classical northern temperate shelf ecosystem. Deep-Sea Res. II 56, 2520–2536.
Howell-Kubler, A.N., Lessard, E.J., Napp, J.M., 1996. Springtime microprotozoan abundance and biomass in the southeastern Bering Sea and Shelikof Strait, Alaska. J. Plankton Res. 18, 731–745.
Hutchins, D.A., DiTullio, G.R., Zhang, Y., Bruland, K.W., 1998. An iron limitation mosaic in the California upwellng regime. Limnol. Oceanogr. 43, 1037–1054.
Jackson, D.A., 1993. Stopping rules in principal components analysis: a comparison of heuristical and statistical approaches. Ecology 74, 2204–2214.
Jacobson, D.M., Anderson, D.M., 1993. Growth and grazing rates of *Protoperidinium hirobis* Abe, a thecate heterotrophic dinoflagellate. J. Plankton Res. 15, 723–726.
Johnson, K.S., Chavez, F.P., Friederich, G.E., 1999. Continental-shelf sediment as a primary source of iron for coastal phytoplankton. Nat. Geosci. 398, 697–700.
Jonasdottir, S.H., 1989. Effects of food concentration on egg-production rates of two species of *Pseudocalanus*: laboratory observations. J. Exp. Mar. Biol. Ecol. 130, 33–43.
Ladd, C., 2007. Interannual variability of the Gulf of Alaska eddy field. Geophys. Res. Lett. 34. https://doi.org/10.1029/2007GL029478.
Ladd, C., Cheng, W., 2016. Gap winds and their effects on regional oceanography Part I: cross sound, Alaska. Deep-Sea Res. II 132, 41–53.
Li, K., Doubleday, A.J., Galbraith, M.D., Hopcroft, R.R., 2016. High abundance of salps in the coastal Gulf of Alaska during 2011: a first record of bloom occurrence for the northern Gulf. Deep-Sea Res. II 132, 136–145.
Liu, H., Dagg, M., Strom, S.L., 2005. Grazing by the calanoid copepod *Neocalanus cristatus* on the microbial foodweb in the coastal Gulf of Alaska. J. Plankton Res. 27, 647–662.
Menden-Deuer, S., Lessard, E.J., 2000. Carbon to volume relationships for dinoflagellates, diatoms, and other protist plankton. Limnol. Oceanogr. 45, 569–579.
Montagnes, D.J.S., Dower, J.F., Figueiredo, G.M., 2010. The protozooplankton-ichthyoplankton trophic link: an overlooked aspect of aquatic food webs. J. Euk. Microbiol. 57, 223–228.
Olson, M.B., Strom, S.L., 2002. Phytoplankton growth, microzooplankton herbivory and community structure in the southeast Bering Sea: insight into the formation and temporal persistence of an *Emiliania huxleyi* bloom. Deep-Sea Res. II 49, 5969–5990.
Pinchuk, A.I., Hopcroft, R.R., 2006. Egg production and ealy development of *Thysanoessa inermis* and *Euphausia pacifica* (Crustacea: euphausiacea) in the northern Gulf of Alaska. J. Exp. Mar. Biol. Ecol. 332, 206–215.
Pinchuk, A.I., Hopcroft, R.R., 2007. Seasonal variations in the growth rates of euphausiids (*Thysanoessa inermis*, *T. spinifera*, and *Euphausia pacifica*) from the northern Gulf of Alaska. Mar. Biol. 151, 257–269.
Putt, M., Stoecker, D.K., 1989. An experimentally determined carbon:volume ratio for marine "oligotrichous" ciliates from estuarine and coastal waters. Limnol. Oceanogr. 34, 1097–1103.
Roff, J.C., Hopcroft, R.R., 1986. High precision microcomputer based measuring system for ecological research. Can. J. Fish. Aquat. Sci. 43, 2044–2048.
Ruzicka, J.J., Steele, J.H., Gaichas, S.K., Ballerinie, T., Gifford, D.J., Brodeur, R.D., Hofmann, E.E., 2013. Analysis of energy flow in US GLOBEC ecosystems using end-to-end models. Oceanography 26, 82–97.
Saito, H., Ota, T., Suzuki, K., Nishioka, J., Tsuda, A., 2006. Role of heterotrophic dinoflagellate *Gyrodinium* sp. in the fate of an iron induced diatom bloom. Geophys. Res. Lett. 33. https://doi.org/10.1029/2005GL025366.
Saiz, E., Calbet, A., 2011. Copepod feeding in the ocean: scaling patterns, composition of their diet and the bias of estimates due to microzooplankton grazing during incubations. Hydrobiologia 666, 181–196.
Schmoker, C., Hernandez-León, S., Calbet, A., 2013. Microzooplankton grazing in the oceans: impacts, data variability, knowledge gaps and future directions. J. Plankton Res. 35, 691–706.
Sherr, E.B., Sherr, B.F., 2007. Heterotrophic dinoflagellates: a significant component of microzooplankton biomass and major grazers of diatoms in the sea. Mar. Ecol. Prog. Ser. 352, 187–197.
Sherr, E.B., Sherr, B.F., McDaniel, J., 1991. Clearance rates of < 6 um fluorescently labeled algae (FLA) by estuarine protozoa: grazing impact of flagellates and ciliates. Mar. Ecol. Prog. Ser. 69, 81–92.
Sherr, E.B., Sherr, B.F., Ross, C., 2013. Microzooplankton grazing impact in the Bering Sea during spring sea ice conditions. Deep-Sea Res. II 94, 57–67.
Stabeno, P.J., Bond, N.A., Hermann, A.J., Kachel, N.B., Mordy, C.W., Overland, J.E., 2004. Meteorology and oceanography of the Northern Gulf of Alaska. Cont. Shelf Res. 24, 859–897.
Stabeno, P.J., Bond, N.A., Kachel, N.B., Ladd, C., Mordy, C.W., Strom, S.L., 2016. Southeast Alaskan shelf from southern tip of Baranof Island to Kayak Island: currents, mixing and chlorophyll-*a*. Deep-Sea Res. II 132, 6–23.
Stoecker, D.K., 2013. Predators of tintinnids. In: Dolan, J.R., Montagnes, D.J.S., Agatha, S., Coats, D.W., Stoecker, D.K. (Eds.), The Biology and Ecology of Tintinnid Ciliates. John Wiley & Sons, Ltd., pp. 122–144.
Stoecker, D.K., Capuzzo, J.M., 1990. Predation on protozoa: its importance to zooplankton. J. Plankton Res. 12, 891–908.
Stoecker, D.K., Weigel, A., Stockwell, D.A., Lomas, M.W., 2014. Microzooplankton: abundance, biomass and contribution to chlorophyll in the Eastern Bering Sea in summer. Deep-Sea Res. II 109, 134–144.
Strom, S.L., 1991. Growth and grazing rates of the herbivorous dinoflagellate *Gymnodinium* sp. from the open subarctic Pacific Ocean. Mar. Ecol. Prog. Ser. 78, 103–113.
Strom, S.L., Brainard, M.A., Holmes, J., Olson, M.B., 2001. Phytoplankton blooms are strongly impacted by microzooplankton grazing in coastal North Pacific waters. Mar. Biol. 138, 355–368.
Strom, S.L., Fredrickson, K.A., 2008. Intense stratification leads to phytoplankton nutrient limitation and reduced microzooplankton grazing in the southeastern Bering Sea. Deep-Sea Res. II 55, 1761–1774.
Strom, S.L., Fredrickson, K.A., Bright, K.J., 2016. Spring phytoplankton in the eastern coastal Gulf of Alaska: photosynthesis and production in high and low bloom years. Deep-Sea Res. II 132, 107–121.
Strom, S.L., Macri, E.L., Fredrickson, K.A., 2010. Light limitation of summer primary production in the coastal Gulf of Alaska: physiological and environmental causes. Mar. Ecol. Prog. Ser. 402, 45–57.
Strom, S.L., Macri, E.L., Olson, M.B., 2007. Microzooplankton grazing in the coastal Gulf of Alaska: variations in top-down control of phytoplankton. Limnol. Oceanogr. 52, 1480–1494.
Strom, S.L., Olson, M.B., Macri, E.L., Mordy, C.W., 2006. Cross-shelf gradients in phytoplankton community structure, nutrient utilization, and growth rate in the coastal Gulf of Alaska. Mar. Ecol. Prog. Ser. 328, 75–92.
Verity, P.G., Villareal, T.A., 1986. The relative food value of diatoms, dinoflagellates, flagellates, and cyanobacteria for tintinnid ciliates. Arch. Protistenkd. 131, 71–84.
Verity, P.G., Robertson, C.Y., Tronzo, C.R., Andrews, M.G., Nelson, J.R., Sieracki, M.E., 1992. Relationships between cell volume and the carbon and nitrogen content of marine photosynthetic nanoplankton. Limnol. Oceanogr. 37, 1434–1446.
Waite, J.N., Mueter, F.J., 2013. Spatial and temporal variability of chlorophyll-*a* concentrations in the coastal Gulf of Alaska, 1998–2011, using cloud-free reconstructions of SeaWiFS and MODIS-Aqua data. Prog. Oceanogr. 116, 179–192.
Weingartner, T.J., 2005. Physical and geological oceanography: coastal boundaries and coastal and ocean circulation. In: Mundy, P.R. (Ed.), The Gulf of Alaska: Biology and Oceanography. Alaska Sea Grant College Program, Fairbanks, pp. 35–48.
Wu, J., Aguilar-Islas, A., Rember, R., Weingartner, T.J., Danielson, S., Whitledge, T.E., 2009. Size-fractionated iron distribution on the northern Gulf of Alaska. Geophys. Res. Lett. 36, L11606 (doi:11610.11029/12009GL038304).